An insight into the effects of electrostatic potentials on the conversion mechanism of the hydrogen-bonded complexes and carbon-bonded complexes: an ab initio and QTAIM investigation

Runtian Chu[a], Yanli Zeng[a,b,*], Mengyu Liu[a], Shijun Zheng[a], Lingpeng Meng[a,*]

[a] Institute of Computational Quantum Chemistry, College of Chemistry and Material Science, Hebei Normal University, Shijiazhuang 050024, P. R. China

[b] National Demonstration Center for Experimental Chemistry Education (Hebei Normal University) , Shijiazhuang 050024, P. R. China

E-mail: yanlizeng@hebtu.edu.cn; menglp@hebtu.edu.cn

Table S1 Energy decomposition analysis of the interaction energies.

	ES	EX	REP	POL	DISP
$CH_3F\cdots HCN$	-5.08	-3.24	5.91	-1.11	0.09
$SiH_3F\cdots HCN$	-7.14	-7.31	13.32	-2.27	-0.60
$GeH_3F\cdots HCN$	-8.56	-9.67	17.74	-3.06	-0.54
$SnH_3F\cdots HCN$	-10.21	-12.44	22.97	-4.02	-0.40
$HCN\cdots CH_3F$	-2.40	-2.77	4.57	-0.38	-0.93
$HCN\cdots SiH_3F$	-4.85	-8.32	14.03	-1.49	-2.20
$HCN\cdots GeH_3F$	-5.35	-8.89	15.17	-1.54	-2.06
$HCN\cdots SnH_3F$	-7.75	-11.99	20.8	-2.54	-2.12

Table S2 Topological characteristics of the BCPs and RCPs for the $CH_3F\cdots HCN \rightarrow$CF-TS$\rightarrow HCN\cdots CH_3F$ IRC path.

Bond	S	ρ_b	λ_1	λ_2	λ_3	$\nabla^2\rho_b$	V_b	G_b	$-G_b/V_b$
F-H									
	$CH_3F\cdots HCN$	0.0144	-0.0175	-0.0168	0.0870	0.0526	-0.0118	0.0125	1.0580
	-24.04	0.0172	-0.0218	-0.0209	0.1048	0.0621	-0.0142	0.0149	1.0451
	-21.07	0.0179	-0.0227	-0.0218	0.1070	0.0624	-0.0149	0.0153	1.0226
	-18.01	0.0163	-0.0197	-0.0194	0.0950	0.0559	-0.0139	0.0139	1.0019
	-16.49	0.0143	-0.0165	-0.0161	0.0831	0.0506	-0.0122	0.0124	1.0183
	-15.88	0.0132	-0.0149	-0.0141	0.0775	0.0484	-0.0112	0.0116	1.0416
	-14.96	0.0114	-0.0124	-0.0109	0.0687	0.0454	-0.0094	0.0104	1.1067
	-13.44	0.0090	-0.0088	-0.0056	0.0556	0.0412	-0.0066	0.0084	1.2823
F-C									
	-12.54	0.0076	-0.0066	-0.0037	0.0450	0.0347	-0.0051	0.0069	1.3595
	-12.23	0.0068	-0.0057	-0.0034	0.0397	0.0306	-0.0044	0.0060	1.3759
	-11.93	0.0061	-0.0049	-0.0032	0.0351	0.0270	-0.0038	0.0053	1.3899
	-10.39	0.0037	-0.0027	-0.0015	0.0202	0.0161	-0.0021	0.0030	1.4708
	-10.09	0.0034	-0.0024	-0.0011	0.0182	0.0148	-0.0019	0.0028	1.4864
	-9.78	0.0031	-0.0021	-0.0004	0.0162	0.0138	-0.0017	0.0026	1.4959
RCP									
	-12.23	0.0045	-0.0015	0.0012	0.0198	0.0196	-0.0024	0.0036	1.5347
	-11.93	0.0044	-0.0017	0.0019	0.0019	0.0194	-0.0024	0.0036	1.5308
	-10.39	0.0035	-0.0019	0.0017	0.0160	0.0158	-0.0020	0.0030	1.4960
	-10.09	0.0033	-0.0019	0.0012	0.0156	0.0149	-0.0019	0.0028	1.4923
	-9.78	0.0031	-0.0019	0.0004	0.0154	0.0139	-0.0017	0.0026	1.4929
	-5.80	0.0046	-0.0032	0.0001	0.0207	0.0176	-0.0023	0.0034	1.4397
	-2.74	0.0047	-0.0035	0.0004	0.0214	0.0182	-0.0024	0.0035	1.4488
	0.00	0.0039	-0.0028	0.0003	0.0176	0.0151	-0.0020	0.0029	1.4595
	+1.82	0.0051	-0.0039	0.0007	0.0237	0.0205	-0.0027	0.0039	1.4457
	+3.87	0.0056	-0.0042	0.0008	0.0264	0.0230	-0.0031	0.0044	1.4381
	+4.89	0.0058	-0.0043	0.0007	0.0279	0.0243	-0.0033	0.0047	1.4306
	+5.10	0.0058	-0.0043	0.0007	0.0282	0.0246	-0.0033	0.0047	1.4289

	+5.30	0.0059	-0.0043	0.0007	0.0285	0.0248	-0.0034	0.0048	1.4269
	+5.50	0.0059	-0.0043	0.0006	0.0288	0.0251	-0.0034	0.0048	1.4246
Bond	***S***	ρ_b	λ_1	λ_2	λ_3	$\nabla^2\rho_b$	V_b	G_b	$-G_b/V_b$
	+5.71	0.0060	-0.0042	0.0006	0.0290	0.0254	-0.0034	0.0049	1.4223
	+5.91	0.0060	-0.0042	0.0006	0.0293	0.0257	-0.0035	0.0050	1.4195
	+6.94	0.0062	-0.0038	0.0002	0.0309	0.0273	-0.0038	0.0053	1.4058
C-N									
	-12.23	0.0046	-0.0010	-0.0009	0.0195	0.0177	-0.0022	0.0033	1.4884
	-11.93	0.0045	-0.0014	-0.0007	0.0191	0.0170	-0.0022	0.0032	1.4587
	-10.39	0.0045	-0.0024	-0.0004	0.0191	0.0163	-0.0022	0.0032	1.4112
	-10.09	0.0045	-0.0025	-0.0003	0.0192	0.0164	-0.0023	0.0032	1.4112
	-9.78	0.0045	-0.0026	-0.0003	0.0194	0.0165	-0.0023	0.0032	1.4120
	-9.48	0.0045	-0.0027	-0.0003	0.0195	0.0166	-0.0023	0.0032	1.4139
	-9.17	0.0045	-0.0027	-0.0002	0.0197	0.0167	-0.0023	0.0032	1.4158
	-8.86	0.0045	-0.0028	-0.0002	0.0198	0.0168	-0.0023	0.0032	1.4187
	-7.33	0.0046	-0.0031	0.0000	0.0204	0.0173	-0.0023	0.0033	1.4304
	-6.72	0.0046	-0.0032	0.0000	0.0206	0.0174	-0.0023	0.0033	1.4338
	-5.80	0.0046	-0.0033	-0.0002	0.0209	0.0175	-0.0023	0.0034	1.4312
	-2.74	0.0047	-0.0035	-0.0006	0.0221	0.0180	-0.0025	0.0035	1.4163
	+5.71	0.0060	-0.0043	-0.0010	0.0299	0.0246	-0.0034	0.0048	1.3912
	+5.91	0.0060	-0.0043	-0.0010	0.0302	0.0249	-0.0035	0.0049	1.3920
	+6.94	0.0062	-0.0039	-0.0004	0.0312	0.0268	-0.0037	0.0052	1.3968
	+7.96	0.0064	-0.0032	-0.0002	0.0321	0.0287	-0.0040	0.0056	1.3951
	+8.98	0.0064	-0.0027	-0.0005	0.0324	0.0291	-0.0041	0.0057	1.3912
	+9.99	0.0063	-0.0024	-0.0007	0.0319	0.0289	-0.0041	0.0056	1.3898
	$HCN\cdots CH_3F$	0.0062	-0.0014	-0.0014	0.0312	0.0285	-0.0040	0.0056	1.3897
H-N									
	0.00	0.0039	-0.0028	-0.0005	0.0182	0.0149	-0.0020	0.0029	1.4329
	+1.82	0.0052	-0.0040	-0.0011	0.0250	0.0199	-0.0028	0.0039	1.3910
	+3.87	0.0056	-0.0043	-0.0013	0.0277	0.0221	-0.0031	0.0043	1.3853
	+4.89	0.0058	-0.0044	-0.0012	0.0290	0.0234	-0.0033	0.0046	1.3876
	+5.10	0.0059	-0.0044	-0.0012	0.0292	0.0237	-0.0033	0.0046	1.3885
	+5.30	0.0059	-0.0044	-0.0011	0.0295	0.0240	-0.0034	0.0047	1.3893
	+5.50	0.0059	-0.0044	-0.0011	0.0297	0.0243	-0.0034	0.0047	1.3906

S: reaction coordinate in unit of $(amu)^{1/2}$bohr

Table S3 Topological characteristics of the BCPs and RCPs for the $SiH_3F\cdots HCN \rightarrow SiF\text{-}TS \rightarrow HCN\cdots SiH_3F$ IRC path

Bond	S	ρ_b	λ_1	λ_2	λ_3	$\nabla^2\rho_b$	V_b	G_b	$-G_b/V_b$
F-H									
	$SiH_3F\cdots HCN$	0.0125	-0.0143	-0.0143	0.0771	0.0485	-0.0102	0.0112	1.0929
F-C									
	-20.64	0.0080	-0.0068	-0.0040	0.0463	0.0355	-0.0054	0.0071	1.3262
	-20.09	0.0080	-0.0066	-0.0045	0.0456	0.0344	-0.0054	0.0070	1.3022
	-19.26	0.0072	-0.0058	-0.0042	0.0402	0.0303	-0.0047	0.0061	1.3099
	-18.70	0.0066	-0.0052	-0.0035	0.0363	0.0276	-0.0042	0.0055	1.3247
F-N									
	-17.86	0.0059	-0.0045	-0.0024	0.0314	0.0245	-0.0037	0.0049	1.3296
	-17.31	0.0057	-0.0043	-0.0018	0.0294	0.0234	-0.0036	0.0047	1.3107
	-15.09	0.0061	-0.0046	-0.0016	0.0318	0.0256	-0.0041	0.0052	1.2797
	-13.70	0.0065	-0.0048	-0.0013	0.0330	0.0270	-0.0043	0.0055	1.2820
	-13.15	0.0065	-0.0047	-0.0008	0.0326	0.0271	-0.0043	0.0056	1.2848
RCP									
	-19.26	0.0046	-0.0013	0.0015	0.0172	0.0174	-0.0026	0.0035	1.3413
	-18.70	0.0047	-0.0016	0.0019	0.0180	0.0183	-0.0027	0.0036	1.3449
	-17.86	0.0049	-0.0020	0.0020	0.0197	0.0197	-0.0029	0.0039	1.3436
	-17.31	0.0051	-0.0023	0.0019	0.0209	0.0206	-0.0031	0.0041	1.3406
	-15.09	0.0060	-0.0032	0.0016	0.0260	0.0245	-0.0038	0.0049	1.3140
	-13.70	0.0064	-0.0038	0.0012	0.0288	0.0262	-0.0041	0.0053	1.2971
	-13.15	0.0065	-0.0041	0.0008	0.0300	0.0267	-0.0042	0.0054	1.2922
	-6.16	0.0047	-0.0032	0.0000	0.0189	0.0158	-0.0024	0.0032	1.3359
	-5.31	0.0045	-0.0030	0.0001	0.0180	0.0151	-0.0022	0.0030	1.3560
	-3.91	0.0043	-0.0029	0.0003	0.0170	0.0144	-0.0020	0.0028	1.3828
	-1.11	0.0041	-0.0027	0.0005	0.0163	0.0140	-0.0019	0.0027	1.4094
	0.00	0.0034	-0.0022	0.0004	0.0136	0.0118	-0.0015	0.0022	1.4480
	+2.06	0.0044	-0.0030	0.0007	0.0176	0.0153	-0.0021	0.0030	1.3921
	+4.28	0.0048	-0.0033	0.0007	0.0192	0.0166	-0.0024	0.0033	1.3602
	+6.51	0.0054	-0.0038	0.0007	0.0215	0.0185	-0.0029	0.0037	1.3100
	+8.76	0.0062	-0.0042	0.0006	0.0245	0.0209	-0.0035	0.0044	1.2497

Bond	S	ρ_b	λ_1	λ_2	λ_3	$\nabla^2\rho_b$	V_b	G_b	$-G_b/V_b$
	+9.89	0.0068	-0.0044	0.0004	0.0267	0.0227	-0.0040	0.0048	1.2174
Si-N									
	-19.26	0.0047	-0.0013	-0.0006	0.0176	0.0158	-0.0025	0.0032	1.2895
	-18.70	0.0049	-0.0017	-0.0005	0.0187	0.0164	-0.0026	0.0034	1.2848
	-17.86	0.0052	-0.0022	-0.0005	0.0202	0.0175	-0.0028	0.0036	1.2815
	-17.31	0.0054	-0.0024	-0.0006	0.0213	0.0183	-0.0029	0.0038	1.2778
	-15.09	0.0064	-0.0030	-0.0007	0.0252	0.0215	-0.0036	0.0045	1.2463
	-13.70	0.0070	-0.0033	-0.0008	0.0271	0.0230	-0.0040	0.0049	1.2227
	-13.15	0.0071	-0.0035	-0.0008	0.0277	0.0234	-0.0041	0.0050	1.2151
	-12.32	0.0073	-0.0037	-0.0008	0.0283	0.0238	-0.0042	0.0051	1.2064
	-9.52	0.0066	-0.0040	-0.0004	0.0260	0.0216	-0.0037	0.0045	1.2291
	-8.12	0.0056	-0.0037	-0.0002	0.0224	0.0185	-0.0030	0.0038	1.2772
	-6.72	0.0049	-0.0033	0.0000	0.0197	0.0164	-0.0025	0.0033	1.3212
	+12.69	0.0086	-0.0038	-0.0005	0.0325	0.0283	-0.0056	0.0063	1.1360
	+13.10	0.0091	-0.0039	-0.0007	0.0345	0.0299	-0.0060	0.0067	1.1245
	+15.28	0.0113	-0.0037	-0.0010	0.0405	0.0358	-0.0079	0.0084	1.0646
	$HCN\cdots SiH_3F$	0.0098	-0.0015	-0.0015	0.0353	0.0322	-0.0068	0.0075	1.0880
H-N									
	-6.16	0.0047	-0.0032	-0.0001	0.0190	0.0158	-0.0024	0.0031	1.3396
	-5.31	0.0045	-0.0031	-0.0002	0.0184	0.0151	-0.0022	0.0030	1.3668
	-3.91	0.0043	-0.0029	-0.0004	0.0179	0.0145	-0.0020	0.0028	1.4023
	-1.11	0.0041	-0.0028	-0.0008	0.0178	0.0142	-0.0019	0.0027	1.4339
	0.00	0.0035	-0.0023	-0.0006	0.0148	0.0119	-0.0015	0.0023	1.4733
	+2.06	0.0045	-0.0031	-0.0010	0.0197	0.0156	-0.0021	0.0030	1.4167
	+4.28	0.0049	-0.0034	-0.0011	0.0215	0.0169	-0.0024	0.0033	1.3895
	+6.51	0.0055	-0.0039	-0.0011	0.0238	0.0187	-0.0028	0.0037	1.3451
	+8.76	0.0062	-0.0043	-0.0010	0.0263	0.0210	-0.0034	0.0043	1.2798
	+9.89	0.0068	-0.0045	-0.0005	0.0276	0.0226	-0.0039	0.0048	1.2307
	+10.55	0.0072	-0.0046	-0.0012	0.0297	0.0239	-0.0042	0.0051	1.2204
	+10.99	0.0075	-0.0046	-0.0012	0.0305	0.0248	-0.0044	0.0053	1.2009
	+12.07	0.0084	-0.0047	-0.0016	0.0337	0.0274	-0.0052	0.0060	1.1658

S: reaction coordinate in unit of $(amu)^{1/2}$bohr

Table S4 Topological characteristics of the BCPs and RCPs for the $GeH_3F\cdots HCN \rightarrow GeF\text{-}TS \rightarrow HCN\cdots GeH_3F$ IRC path

Bond	S	ρ_b	λ_1	λ_2	λ_3	$\nabla^2\rho_b$	V_b	G_b	$-G_b/V_b$
F-H									
	$GeH_3F\cdots HCN$	0.0153	-0.0180	-0.0180	0.0947	0.0587	-0.0126	0.0136	1.0816
F-C									
	-26.79	0.0100	-0.0088	-0.0048	0.0577	0.0442	-0.0073	0.0092	1.2602
	-22.02	0.0081	-0.0065	-0.0044	0.0442	0.0333	-0.0054	0.0069	1.2643
	-20.60	0.0074	-0.0058	-0.0035	0.0396	0.0303	-0.0049	0.0062	1.2754
F-N									
	-19.62	0.0068	-0.0051	-0.0022	0.0345	0.0272	-0.0044	0.0056	1.2677
	-18.40	0.0062	-0.0046	-0.0017	0.0311	0.0249	-0.0041	0.0052	1.2560
	-17.25	0.0061	-0.0046	-0.0015	0.0310	0.0250	-0.0041	0.0052	1.2597
	-16.05	0.0063	-0.0046	-0.0009	0.0311	0.0257	-0.0042	0.0053	1.2729
RCP									
	-26.79	0.0056	-0.0018	0.0013	0.0204	0.0199	-0.0031	0.0040	1.3143
	-22.02	0.0058	-0.0028	0.0031	0.0219	0.0222	-0.0034	0.0045	1.3086
	-20.60	0.0059	-0.0030	0.0030	0.0231	0.0231	0.0047	0.0047	1.3017
	-19.62	0.0060	-0.0032	0.0026	0.0246	0.0240	-0.0038	0.0049	1.2989
	-18.40	0.0060	-0.0035	0.0021	0.0256	0.0241	-0.0037	0.0049	1.3049
	-17.25	0.0060	-0.0038	0.0017	0.0268	0.0247	-0.0038	0.0050	1.3035
	-16.05	0.0062	-0.0041	0.0009	0.0289	0.0257	-0.0040	0.0052	1.2938
	-3.84	0.0048	-0.0032	0.0001	0.0191	0.0160	-0.0024	0.0032	1.3493
	-2.34	0.0048	-0.0032	0.0003	0.0191	0.0161	-0.0024	0.0032	1.3547
	0.00	0.0038	-0.0024	0.0003	0.0149	0.0128	-0.0018	0.0025	1.4106
	+4.72	0.0052	-0.0036	0.0004	0.0206	0.0175	-0.0026	0.0035	1.3280
	+7.31	0.0058	-0.0040	0.0003	0.0227	0.0191	-0.0030	0.0039	1.2859
	+8.57	0.0062	-0.0043	0.0002	0.0242	0.0202	-0.0033	0.0042	1.2625

Bond	S	ρ_b	λ_1	λ_2	λ_3	$\nabla^2\rho_b$	V_b	G_b	$-G_b/V_b$
Ge-N									
	-26.79	0.0057	-0.0014	-0.0010	0.0207	0.0183	-0.0030	0.0038	1.2618
	-22.02	0.0063	-0.0034	-0.0016	0.0254	0.0204	-0.0033	0.0042	1.2750
	-20.60	0.0066	-0.0036	-0.0017	0.0267	0.0214	-0.0035	0.0044	1.2679
	-19.62	0.0066	-0.0032	-0.0014	0.0263	0.0218	-0.0037	0.0046	1.2363
	-18.40	0.0067	-0.0034	-0.0014	0.0268	0.0220	-0.0037	0.0046	1.2369
	-17.25	0.0071	-0.0045	-0.0020	0.0297	0.0233	-0.0038	0.0048	1.2712
	-16.05	0.0072	-0.0039	-0.0016	0.0290	0.0235	-0.0041	0.0050	1.2242
	-14.80	0.0078	-0.0044	-0.0017	0.0312	0.0251	-0.0045	0.0054	1.2016
	-12.36	0.0082	-0.0049	-0.0018	0.0327	0.0261	-0.0048	0.0057	1.1822
	-9.82	0.0066	-0.0045	-0.0014	0.0271	0.0211	-0.0034	0.0043	1.2759
	-7.41	0.0056	-0.0037	-0.0004	0.0224	0.0182	-0.0029	0.0037	1.2905
	-4.87	0.0050	-0.0034	0.0000	0.0199	0.0165	-0.0025	0.0033	1.3356
	-3.84	0.0048	-0.0033	-0.0002	0.0196	0.0161	-0.0023	0.0032	1.3628
	+8.57	0.0062	-0.0043	-0.0005	0.0251	0.0203	-0.0032	0.0042	1.2829
	+9.32	0.0064	-0.0044	-0.0007	0.0260	0.0209	-0.0034	0.0043	1.2717
	+9.81	0.0065	-0.0045	-0.0009	0.0267	0.0212	-0.0035	0.0044	1.2672
	+12.27	0.0075	-0.0051	-0.0011	0.0305	0.0242	-0.0042	0.0052	1.2128
	+14.79	0.0090	-0.0053	-0.0015	0.0358	0.0289	-0.0056	0.0064	1.1485
	+19.62	0.0135	-0.0061	-0.0049	0.0554	0.0444	-0.0096	0.0103	1.0800
	HCN···GeH_3F	0.0106	-0.0039	-0.0039	0.0426	0.0347	-0.0071	0.0079	1.1084
H-N									
	-2.34	0.0049	-0.0033	-0.0005	0.0201	0.0163	-0.0023	0.0032	1.3799
	0.00	0.0038	-0.0025	-0.0004	0.0158	0.0129	-0.0017	0.0025	1.4361
	+4.72	0.0053	-0.0037	-0.0009	0.0225	0.0178	-0.0026	0.0035	1.3616
	+7.31	0.0058	-0.0040	-0.0006	0.0239	0.0193	-0.0030	0.0039	1.3134

S: reaction coordinate in unit of $(amu)^{1/2}$bohr

Table S5 Topological characteristics of the BCPs and RCPs for the $SnH_3F\cdots HCN \rightarrow$ SnF-TS$\rightarrow HCN\cdots SnH_3F$ IRC path

Bond	S	ρ_b	λ_1	λ_2	λ_3	$\nabla^2\rho_b$	V_b	G_b	$-G_b/V_b$
F-H									
	$SnH_3F\cdots HCN$	0.0181	-0.0221	-0.0221	0.1128	0.0687	-0.0149	0.0161	1.0743
F-C									
	-33.28	0.0129	-0.0113	-0.0078	0.0715	0.0524	-0.0102	0.0117	1.1398
	-30.27	0.0104	-0.0086	-0.0053	0.0558	0.0420	-0.0076	0.0091	1.1875
	-30.01	0.0100	-0.0081	-0.0047	0.0527	0.0400	-0.0072	0.0086	1.1978
F-N									
	-29.74	0.0099	-0.0079	-0.0041	0.0516	0.0395	-0.0071	0.0085	1.1988
	-29.47	0.0093	-0.0073	-0.0035	0.0479	0.0371	-0.0065	0.0079	1.2092
	-28.40	0.0085	-0.0065	-0.0023	0.0418	0.0330	-0.0060	0.0071	1.1931
	-25.87	0.0085	-0.0065	-0.0022	0.0413	0.0326	-0.0060	0.0071	1.1774
	-23.33	0.0087	-0.0066	-0.0020	0.0417	0.0331	-0.0061	0.0072	1.1760
	-21.05	0.0088	-0.0068	-0.0013	0.0417	0.0336	-0.0062	0.0073	1.1813
RCP									
	-33.28	0.0080	-0.0042	0.0050	0.0279	0.0286	-0.0049	0.0060	1.2233
	-30.27	0.0080	-0.0046	0.0046	0.0292	0.0292	-0.0051	0.0062	1.2152
	-30.01	0.0079	-0.0046	0.0044	0.0289	0.0288	-0.0050	0.0061	1.2169
	-29.74	0.0081	-0.0048	0.0044	0.0302	0.0298	-0.0052	0.0063	1.2113
	-29.47	0.0349	-0.0047	0.0041	0.0297	0.0291	-0.0051	0.0062	1.2158
	-28.40	0.0080	-0.0050	0.0035	0.0313	0.0298	-0.0052	0.0063	1.2145
	-25.87	0.0083	-0.0055	0.0028	0.0340	0.0312	-0.0055	0.0067	1.2057
	-23.33	0.0086	-0.0059	0.0022	0.0358	0.0322	-0.0058	0.0069	1.1994
	-21.05	0.0088	-0.0063	0.0014	0.0380	0.0331	-0.0060	0.0071	1.1933
Sn-N									
	-33.28	0.0088	-0.0040	-0.0029	0.0327	0.0258	-0.0051	0.0058	1.1361
	-30.27	0.0091	-0.0047	-0.0030	0.0346	0.0269	-0.0052	0.0060	1.1414
	-30.01	0.0089	-0.0045	-0.0031	0.0342	0.0266	-0.0052	0.0059	1.1423
	-29.74	0.0092	-0.0047	-0.0033	0.0356	0.0275	-0.0054	0.0061	1.1403
	-29.47	0.0090	-0.0046	-0.0033	0.0349	0.0270	-0.0052	0.0060	1.1433
	-28.40	0.0093	-0.0049	-0.0034	0.0362	0.0279	-0.0054	0.0062	1.1422
	-25.87	0.0099	-0.0055	-0.0037	0.0389	0.0296	-0.0059	0.0066	1.1325
	-23.33	0.0102	-0.0058	-0.0039	0.0403	0.0305	-0.0061	0.0069	1.1256
	-21.05	0.0105	-0.0060	-0.0043	0.0418	0.0315	-0.0064	0.0071	1.1160
	-20.54	0.0106	-0.0062	-0.0043	0.0421	0.0317	-0.0065	0.0072	1.1124
	-19.28	0.0107	-0.0065	-0.0042	0.0426	0.0319	-0.0066	0.0073	1.1070
	-11.43	0.0079	-0.0052	-0.0020	0.0300	0.0228	-0.0044	0.0051	1.1435
	-3.54	0.0054	-0.0035	-0.0003	0.0199	0.0160	-0.0027	0.0034	1.2386
	0.00-TS	0.0042	-0.0026	-0.0001	0.0156	0.0129	-0.0020	0.0026	1.3074
	+5.91	0.0056	-0.0037	-0.0001	0.0204	0.0166	-0.0029	0.0035	1.2230
	+10.06	0.0065	-0.0043	-0.0007	0.0239	0.0190	-0.0035	0.0041	1.1719
	+12.87	0.0080	-0.0051	-0.0016	0.0299	0.0232	-0.0046	0.0052	1.1306
	+16.92	0.0117	-0.0070	-0.0046	0.0473	0.0357	-0.0076	0.0082	1.0886
	+21.41	0.0169	-0.0105	-0.0101	0.0757	0.0551	-0.0126	0.0132	1.0468
	$HCN\cdots SnH_3F$	0.0166	-0.0102	-0.0100	0.0743	0.0540	-0.0123	0.0129	1.0477

S: reaction coordinate in unit of $(amu)^{1/2}$

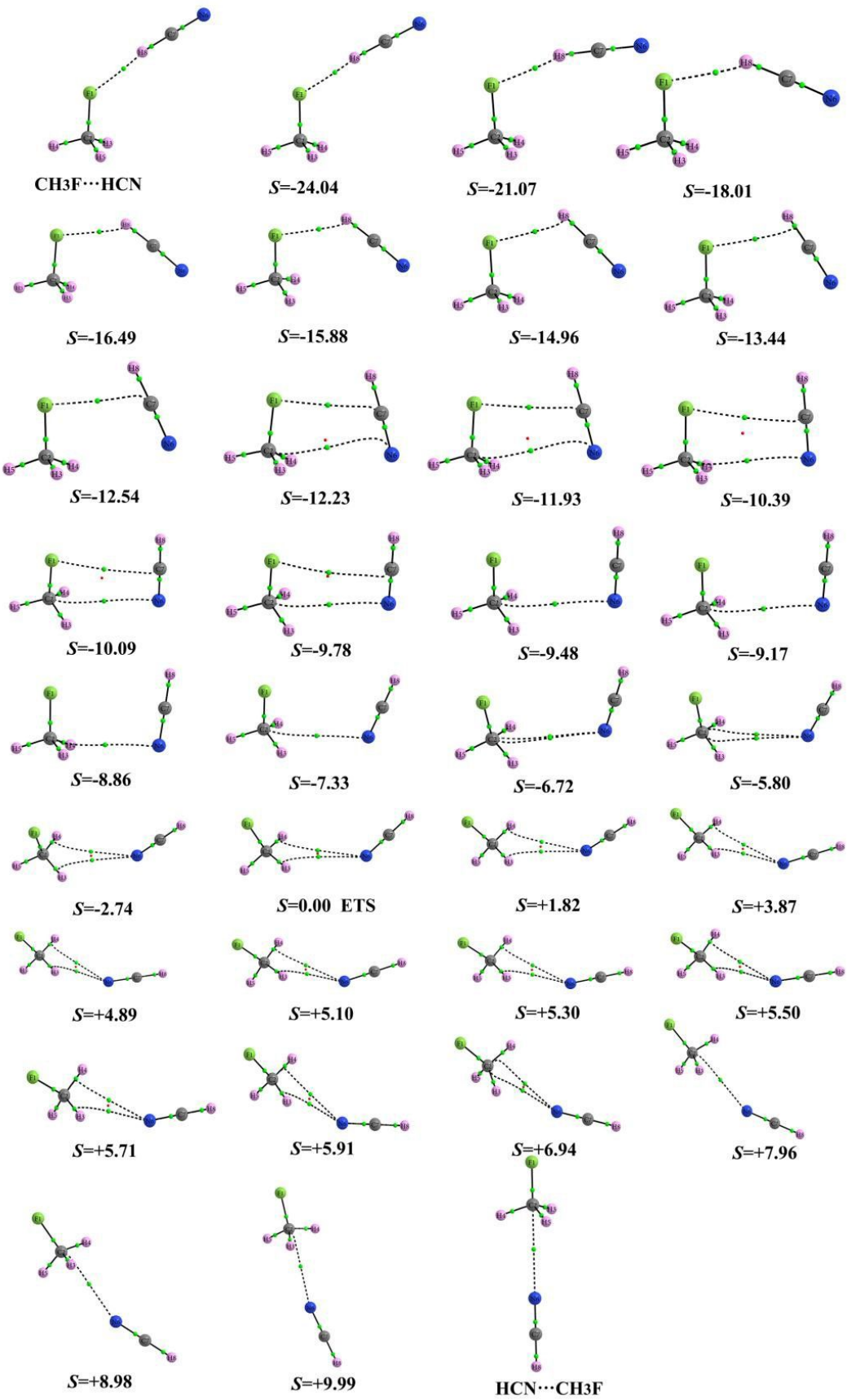

Figure S1 Topological analysis of each stagnation for the $CH_3F\cdots HCN \rightarrow$ CF-TS $\rightarrow$ $HCN\cdots CH_3F$ IRC path

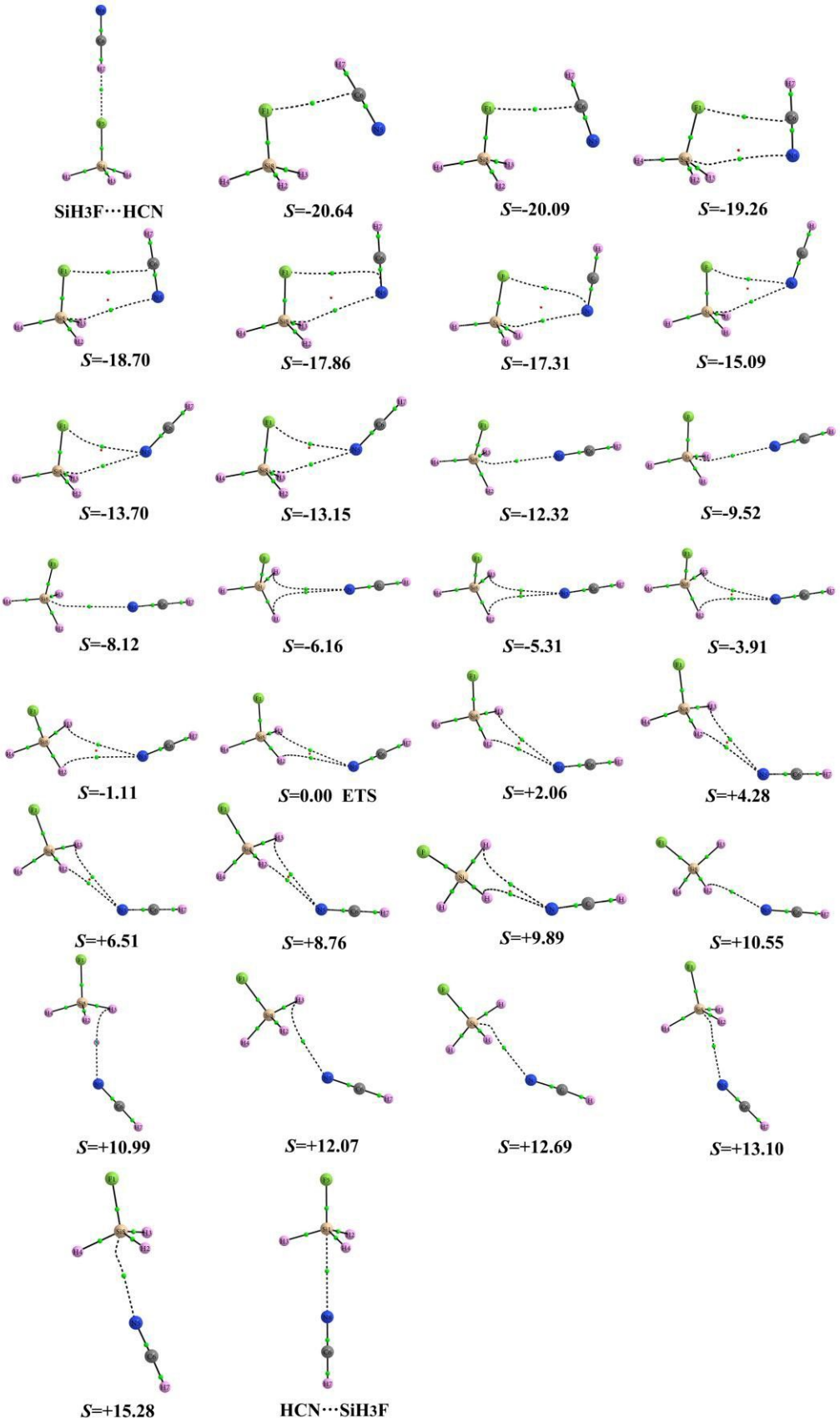

Figure S2 Topological analysis ofeach stagnation for theSiH_3F···HCN→SiF-TS→ HCN···SiH_3F IRC path

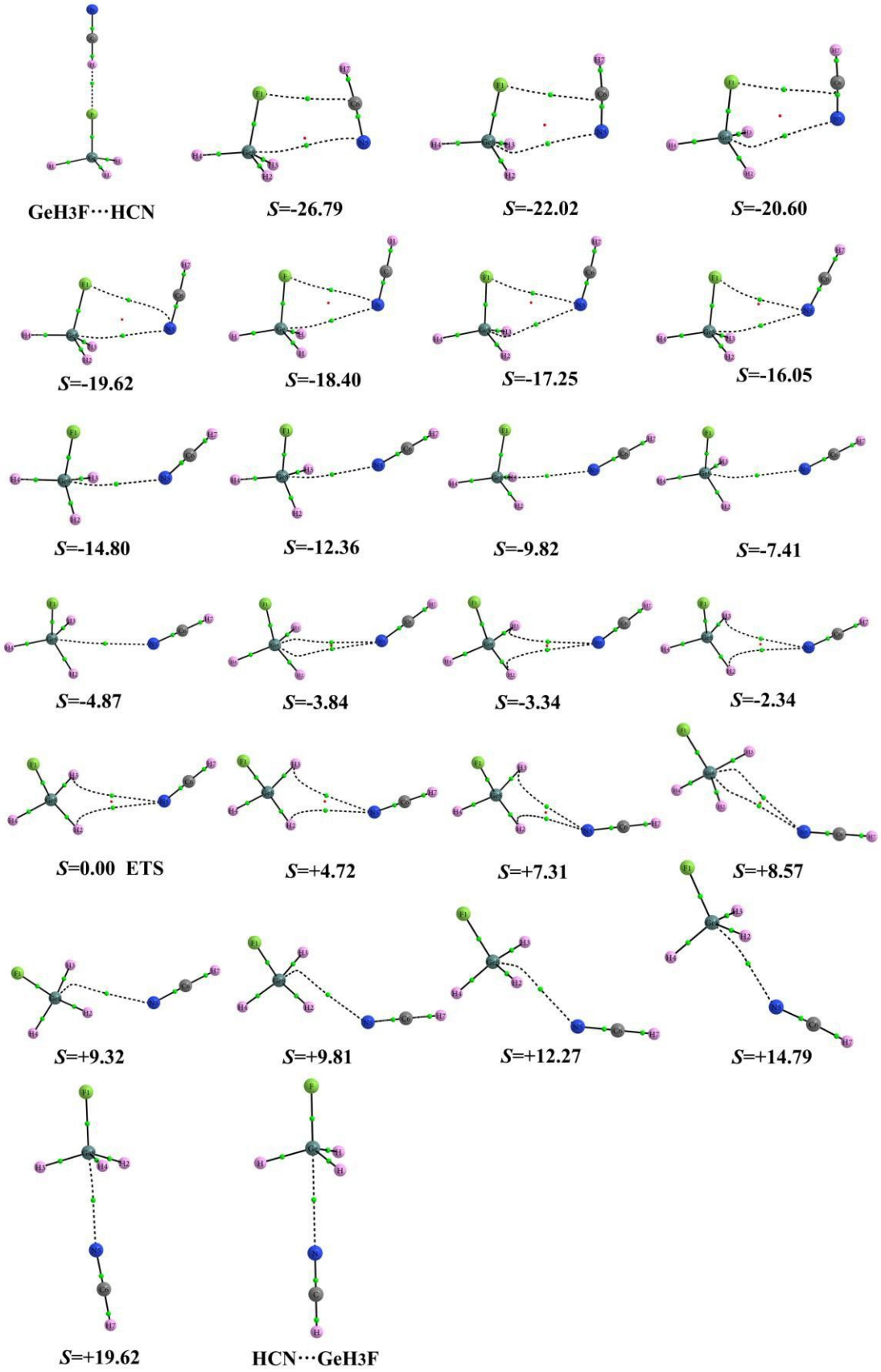

Figure S3 Topological analysis ofeach stagnation for the$GeH_3F\cdots HCN \rightarrow GeF\text{-}TS \rightarrow HCN\cdots GeH_3F$ IRC path

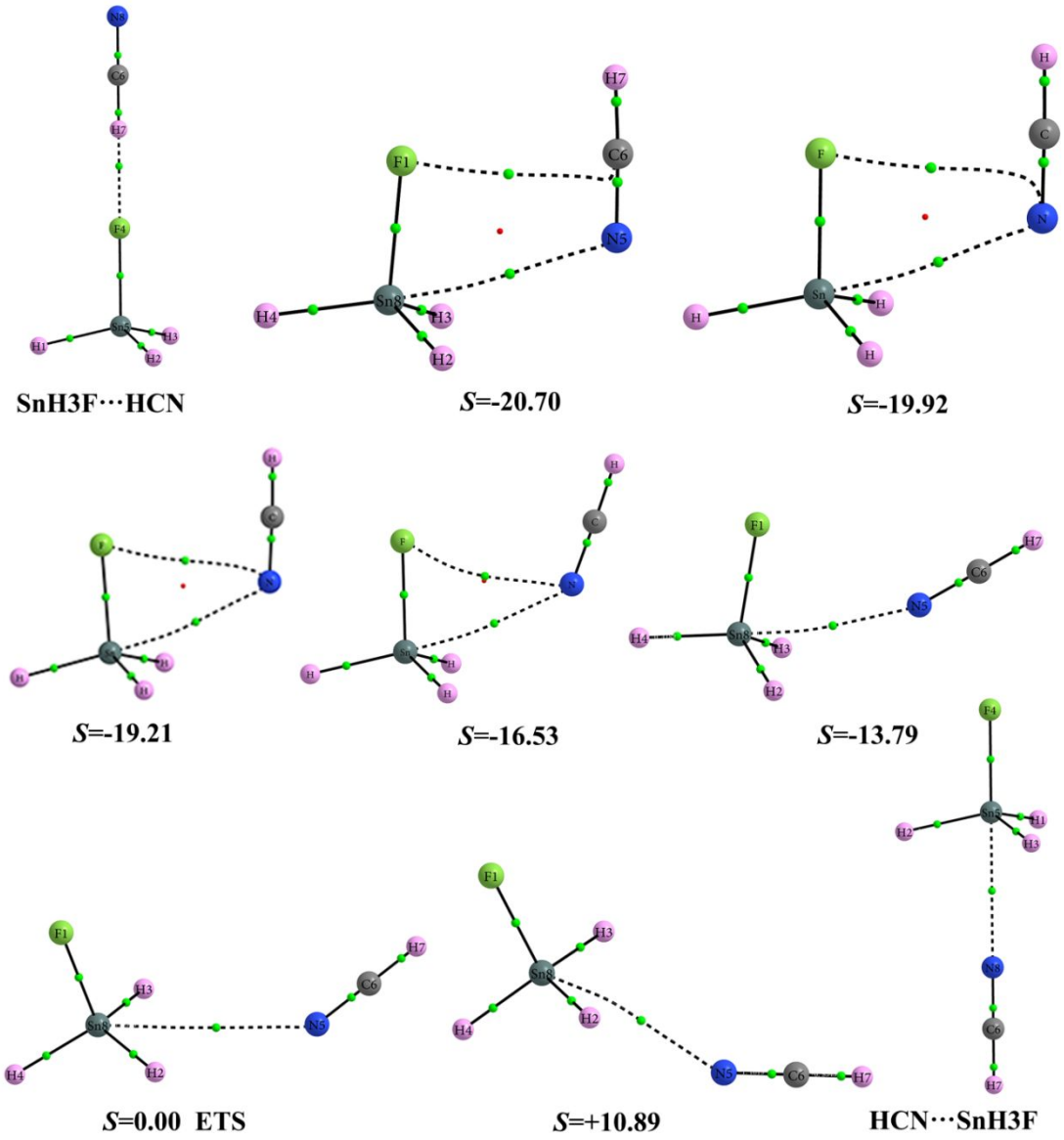

Figure S4 Topological analysis of each stagnation for the $SnH_3F\cdots HCN \rightarrow$ SnF-TS $\rightarrow$ $HCN\cdots SnH_3F$ IRC path